

Pygmies, giants, and skins as laboratory constraints on the equation of state of neutron-rich matter

J. Piekarewicz

Department of Physics, Florida State University, Tallahassee, FL 32306-4350, USA

E-mail: jpiekarewicz@fsu.edu

Abstract. Laboratory experiments sensitive to the density dependence of the symmetry energy may place stringent constraints on the equation of state of neutron-rich matter and, thus, on the structure, dynamics, and composition of neutron stars. Understanding the equation of state of neutron-rich matter is a central goal of nuclear physics that cuts across a variety of disciplines. In this contribution I focus on how laboratory experiments on neutron skins and on both Pygmy and Giant resonances can help us elucidate the structure of neutron stars.

1. Introduction

One of the central questions framing the recent report by The Committee on the Assessment of and Outlook for Nuclear Physics is “*How does subatomic matter organize itself?*” [1]. Remarkably, most of the fascinating phases that are predicted to emerge in this subatomic domain can not be probed under normal laboratory conditions. However, such novel states of matter become stable in the interior of neutron stars by virtue of the enormous gravitational fields. The fascinating phases predicted to exist in the crust of neutron stars, such as Coulomb crystals of neutron-rich nuclei and nuclear pasta, are within the purview of the Facility for Rare Isotope Beams (FRIB) which has as one of its science goals to provide an understanding of matter in the crust of neutron stars [2]. FRIB is of relevance to neutron-star structure because at sub-saturation densities the uniform neutron-rich matter residing in the stellar core becomes unstable against cluster formation. That is, at these sub-saturation densities the separation between nucleons increases to such an extent that it becomes energetically favorable for the system to segregate into regions of normal density (*i.e.*, nuclear clusters) embedded in a dilute, likely superfluid, neutron vapor. This “*clustering instability*” signals the transition from the uniform liquid core to the non-uniform stellar crust (see Fig. 1).

The outer stellar crust of relevance to the FRIB program is comprised of a Coulomb lattice of neutron-rich nuclei immersed in a uniform electron gas [3, 4, 5, 6]). At the lowest densities of the outer crust, the Coulomb lattice is formed from ^{56}Fe nuclei. However, as the density increases—and given that the electronic Fermi energy increases rapidly with density—it becomes energetically favorable for electrons to capture into protons leading to the formation of a Coulomb crystal of progressively more neutron-rich nuclei; a progression that starts with ^{56}Fe and is predicted to terminate with the exotic, neutron-rich nucleus ^{118}Kr (see Fig. 1).

Eventually, the neutron-proton asymmetry becomes too large for the nuclei to bind any more neutrons and the excess neutrons go into the formation of a dilute neutron vapor. However, at inner-crust densities, distance scales that were well separated in both the crystalline phase (where

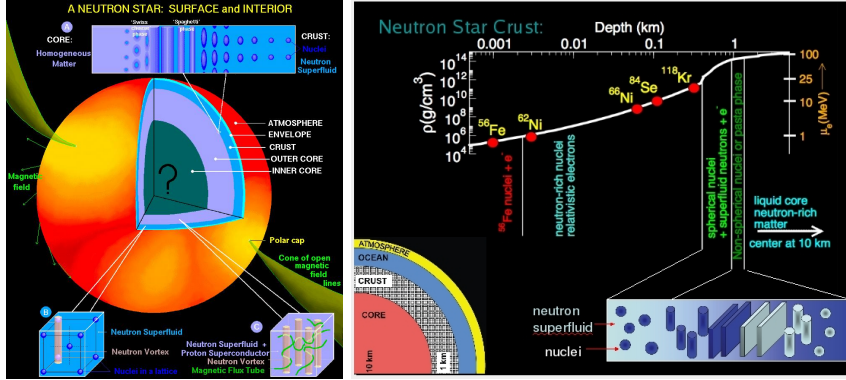


Figure 1. A scientifically-accurate rendition of the structure and phases of a neutron star (courtesy of Dany Page) and the composition of the stellar crust (courtesy of Sanjay Reddy).

the long-range Coulomb interaction dominates) and in the uniform phase (where the short-range strong interaction dominates) become comparable. This gives rise to “*Coulomb frustration*”, a phenomenon characterized by the formation of a myriad of complex structures radically different in topology yet extremely close in energy. Given that these complex structures—collectively referred to as “*nuclear pasta*”—are very close in energy, it has been speculated that the transition from the highly ordered crystal to the uniform phase must proceed through a series of changes in the dimensionality and topology of these structures [7, 8]. Moreover, due to the preponderance of low-energy states, frustrated systems display an interesting and unique low-energy dynamics that has been studied using a variety of techniques including numerical simulations [9, 10, 11, 12, 13, 14].

FRIB will not be the only experimental program of direct relevance to the structure of neutron stars. Indeed, the *Lead Radius EXperiment* (“PREX”) at the Jefferson Laboratory measures the neutron radius of ^{208}Pb . When combining this purely electroweak result with the accurately known charge radius of ^{208}Pb , one obtains its “*neutron skin*”—the difference between the root-mean-square neutron and proton radii. As we shall see later, the neutron skin correlates strongly to the pressure of pure neutron matter at saturation density which, in turn, correlates strongly to the neutron-star radius.

2. Formalism

Neutron stars satisfy the Tolman-Oppenheimer-Volkoff (TOV) equations, which are the extension of Newton’s laws to the domain of general relativity. The TOV equations may be expressed as a coupled set of first-order differential equations of the following form:

$$\frac{dP}{dr} = -G \frac{\mathcal{E}(r)M(r)}{r^2} \left[1 + \frac{P(r)}{\mathcal{E}(r)} \right] \left[1 + \frac{4\pi r^3 P(r)}{M(r)} \right] \left[1 - \frac{2GM(r)}{r} \right]^{-1}, \quad (1)$$

$$\frac{dM}{dr} = 4\pi r^2 \mathcal{E}(r), \quad (2)$$

where G is Newton’s gravitational constant and $P(r)$, $\mathcal{E}(r)$, and $M(r)$ represent the pressure, energy density, and enclosed-mass profiles of the star, respectively. Note that the three terms enclosed in square brackets in Eq. (1) are of general-relativistic origin. Notably, the only input that neutron stars are sensitive to is the equation of state (EOS), namely, $P = P(\mathcal{E})$. In Fig. 2 we display *mass-vs-radius* relations as predicted by three relativistic mean-field models [15]. Surprisingly, all three models—NL3 [16, 17], FSU [18], and IU-FSU [15], are able to

accurately reproduce a variety of ground-state observables throughout the nuclear chart. Yet, the predictions displayed in Fig. 2 are significantly different. A central goal of this contribution is to identify critical laboratory observables that may be used to constrain the structure, dynamics, and composition of neutron stars.

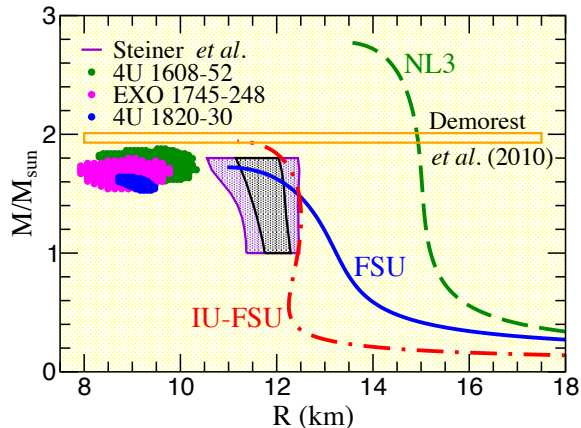


Figure 2. (Color online) *Mass-vs-Radius* relation predicted by the three relativistic mean-field models [15]. The observational data that suggest very small stellar radii represent 1σ confidence contours for the three neutron stars reported in Ref. [19]. The two shaded areas that suggest larger radii are 1σ and 2σ contours extracted from the analysis of Ref. [20]. The seminal measurement of the heaviest neutron star by Demorest et al., is also indicated in the figure [21].

The starting point for the calculation of both nuclear and neutron-star structure is a relativistic energy density functional characterized by the interacting Lagrangian density of Ref. [22] supplemented by an isoscalar-isovector term first introduced in Ref. [23]. That is,

$$\begin{aligned} \mathcal{L}_{\text{int}} = & \bar{\psi} \left[g_s \phi - \left(g_v V_\mu + \frac{g_\rho}{2} \boldsymbol{\tau} \cdot \mathbf{b}_\mu + \frac{e}{2} (1 + \tau_3) A_\mu \right) \gamma^\mu \right] \psi \\ & - \frac{\kappa}{3!} (g_s \phi)^3 - \frac{\lambda}{4!} (g_s \phi)^4 + \frac{\zeta}{4!} g_v^4 (V_\mu V^\mu)^2 + \Lambda_v \left(g_\rho^2 \mathbf{b}_\mu \cdot \mathbf{b}^\mu \right) \left(g_v^2 V_\nu V^\nu \right). \end{aligned} \quad (3)$$

The Lagrangian density includes an isodoublet nucleon field (ψ) interacting via the exchange of two isoscalar mesons, a scalar (ϕ) and a vector (V^μ), one isovector meson (b^μ), and the photon (A^μ) [24, 25]. In addition to meson-nucleon interactions, the Lagrangian density is supplemented by four nonlinear meson interactions with coupling constants (κ , λ , ζ , and Λ_v) that are included primarily to soften the equation of state of both symmetric nuclear matter and pure neutron matter. For a detailed discussion on the impact of these terms on various quantities of theoretical, experimental, and observational interest see Ref. [26].

Laboratory experiments may play a critical role in constraining the size of neutron stars because stellar radii are controlled by the density dependence of the symmetry energy in the immediate vicinity of nuclear-matter saturation density [27]. Recall that the symmetry energy may be viewed as the difference in the energy between pure neutron matter and symmetric nuclear matter. A particularly critical property of the symmetry energy that is poorly constrained is its slope at saturation density—a quantity customarily denoted by L and closely related to the pressure of pure neutron matter [28]. Although L is not directly observable, it is strongly correlated to the thickness of the neutron skin of heavy nuclei [29, 30]. As indicated in the left-hand panel of Fig. 3, the thickness of the neutron skin depends sensitively on the pressure of neutron-rich matter: *the greater the pressure the thicker the neutron skin*. And it

is exactly this same pressure that supports neutron stars against gravitational collapse. Thus, as indicated in the right-hand panel of Fig. 3, models with thicker neutron skins often produce neutron stars with larger radii [23, 31]. Thus, it is possible to study “data-to-data” relations between the neutron-rich skin of a heavy nucleus and the radius of a neutron star.

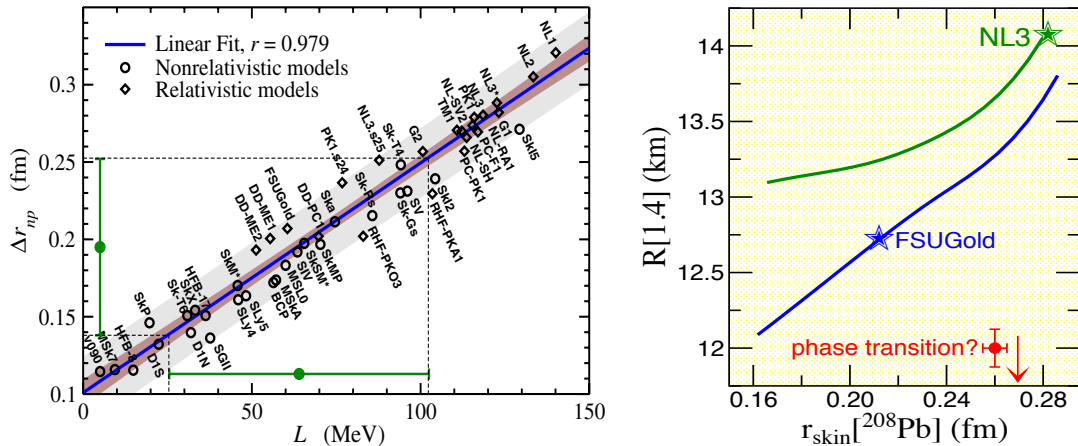


Figure 3. (Color online) The left-hand panel displays the correlation between the neutron-skin of ^{208}Pb and the slope of the symmetry energy for a variety of nonrelativistic and relativistic models [32]. The right-hand panel shows the correlation between the neutron-skin of ^{208}Pb and the radius of a $1.4 M_{\odot}$ neutron star for two relativistic mean-field models.

3. Neutron Skins: The Lead Radius Experiment (PREX)

The successfully commissioned Lead Radius Experiment has provided the first model-independent evidence of the existence of a significant neutron skin in ^{208}Pb [33, 34]. Parity violation at low momentum transfers is particularly sensitive to the neutron distribution because the neutral weak-vector boson (Z^0) couples preferentially to the neutrons in the target [35]. Although PREX achieved the systematic control required to perform this challenging experiment, unforeseen technical problems resulted in time losses that significantly compromised the statistical accuracy of the measurement. This resulted in the following value for the neutron-skin thickness of ^{208}Pb [33, 34]:

$$r_{\text{skin}} = R_n - R_p = 0.33^{+0.16}_{-0.18} \text{ fm}. \quad (4)$$

Given that the determination of the neutron radius of a heavy nucleus is a problem of fundamental importance with far reaching implications in areas as diverse as nuclear structure [29, 30, 36, 37, 38], atomic parity violation [39, 40], heavy-ion collisions [41, 42, 43, 44, 45], and neutron-star structure [23, 31, 46, 47, 48, 49, 50], the PREX collaboration has made a successful proposal for additional beam time so that the original 1% goal (or ± 0.05 fm) may be attained [51]. While the scientific case for such a critical experiment remains strong, the search for additional physical observables that may be both readily accessible and strongly correlated to the neutron skin (and thus also to L) is a worthwhile enterprise. It is precisely the exploration of such a correlation between the *electric dipole polarizability* and the neutron-skin thickness of ^{208}Pb that is at the center of the next section.

4. Pygmies and Giant Resonances

A promising complementary approach to the parity-violating program relies on the electromagnetic excitation of the electric dipole mode [52]. For this mode of excitation—

perceived as a collective oscillation of neutrons against protons—the symmetry energy acts as the restoring force. In particular, models with a soft symmetry energy predict large values for the symmetry energy at the densities of relevance to the excitation of this mode. As a consequence, the stronger restoring force of the softer models generates a dipole response that is both hardened and quenched relative to its stiffer counterparts. In particular, the *inverse* energy-weighted sum, which is directly proportional to the electric dipole polarizability α_D , is highly sensitive to the density dependence of the symmetry energy [53]. This sensitivity suggests the existence of the following interesting correlation in heavy nuclei: *the larger r_{skin} the larger α_D* .

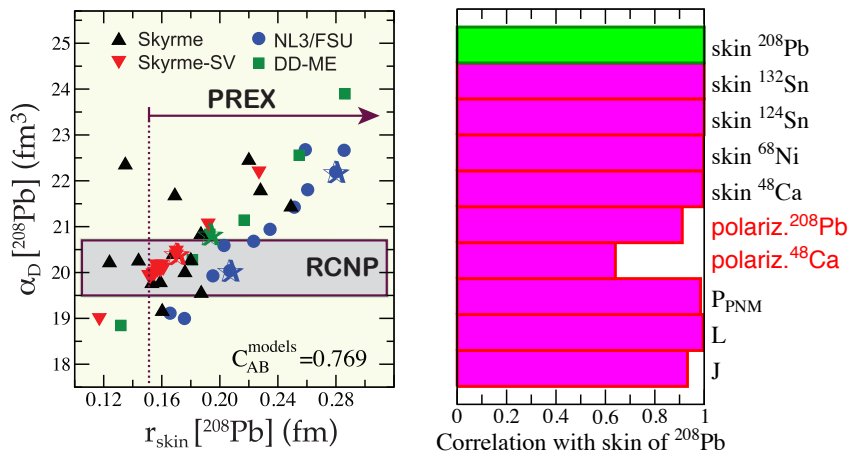


Figure 4. (Color online) Predictions from a variety of nuclear models for the electric dipole polarizability and neutron-skin thickness of ^{208}Pb are shown on the left-hand side of the figure. Also shown are constraints on the neutron-skin thickness from PREX [33, 34] and on the dipole polarizability from RCNP [55, 56]. On the right-hand side of the figure we show correlation coefficients between the neutron-skin thickness of ^{208}Pb and several observables as obtained from a covariance analysis based on the FSU interaction [59].

To test the validity of this correlation we display on the left-hand panel of Fig. 4 α_D in ^{208}Pb as a function of its corresponding neutron-skin as predicted by a large number (48) of nuclear-structure models [54]. From the distribution of electric dipole strength (R_{E1}) the dipole polarizability is readily extracted from the inverse energy-weighted sum. That is,

$$\alpha_D = \frac{8\pi}{9} e^2 \int_0^\infty \omega^{-1} R_{E1}(\omega) d\omega . \quad (5)$$

At first glance a clear (positive) correlation between the dipole polarizability and the neutron skin is discerned. However, on closer examination one observes a significant scatter in the results—especially in the case of the standard Skyrme forces (denoted by the black triangles). In particular, by including the predictions from all the 48 models under consideration, a correlation coefficient of 0.77 was obtained. Also shown in the figure are experimental constraints imposed from PREX and the recent high-resolution measurement of α_D in ^{208}Pb [55, 56]. By imposing these recent experimental constraints, several of the models—especially those with either a very soft or very stiff symmetry energy—may already be ruled out.

However, to establish how the dipole polarizability may provide a unique constraint on the neutron-skin thickness of neutron-rich nuclei and other isovector observables we display on the right-hand panel of Fig. 4 correlation coefficients computed using a single underlying model, namely, FSU [18]. For details on the implementation of the required covariance analysis we refer

the reader to Refs. [57, 58, 59]. According to the model, an accurate measurement of the neutron skin-thickness in ^{208}Pb significantly constrains the neutron skin on a variety of other neutron-rich nuclei. Moreover, the correlation coefficient between the neutron skin and α_D in ^{208}Pb is very large (of about 0.9). This suggests that a multi-prong approach consisting of combined measurements of both neutron skins and α_D —ideally on a variety of nuclei—should significantly constrain the isovector sector of the nuclear energy density functional as well as the EOS of neutron-rich matter.

Naturally, a more stringent constrain on the isovector sector of the nuclear density functional is expected to emerge along an isotopic chain as the nucleus develops a neutron-rich skin. Concomitant with the development of a neutron skin one expects the emergence of low energy dipole strength—the so-called *pygmy dipole resonance* [60, 61, 62, 63, 64, 65, 66]. Thus, it has been suggested that the pygmy dipole resonance (PDR)—speculated to be an excitation of the neutron-rich skin against the isospin symmetric core—may be used as a constraint on the neutron skin [67].

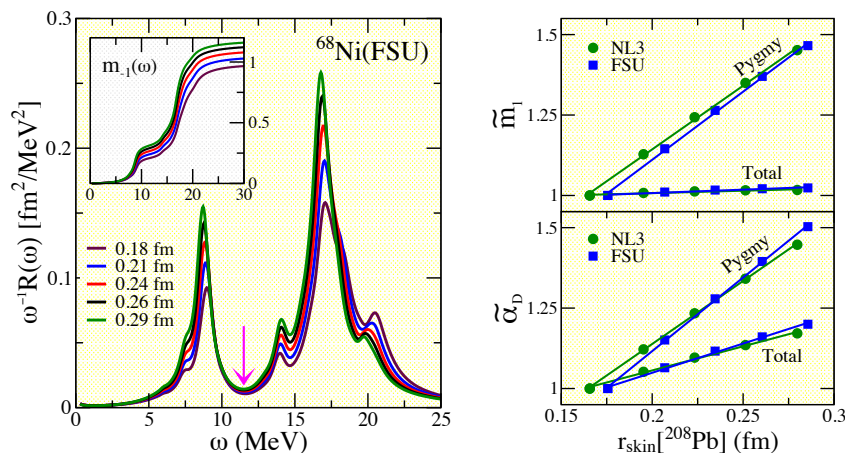


Figure 5. (Color online) The inverse energy weighted dipole response in ^{68}Ni computed with the FSU family of effective interactions is shown on the left-hand side of the figure. The inset displays the running sum. The arrow indicates the (ad-hoc) energy at which the low-energy (pygmy) response is separated from the high-energy (giant) response. On the right-hand side the fractional change in the energy weighted sum and dipole polarizability for ^{68}Ni are displayed as a function of the neutron-skin thickness of ^{208}Pb . See Ref. [53] for more details.

In particular, the fraction of the *inverse energy weighted sum rule* concentrated on the low-energy region appears to be sensitive to the neutron skin of neutron-rich nuclei. The inverse energy weighted response $\omega^{-1}R(\omega)$ is displayed on the left-hand panel of Fig. 5 for the neutron-rich nucleus ^{68}Ni . Given that the ω^{-1} factor enhances the low-energy part of response, the Pygmy resonance accounts for a significant fraction (of about 20-25%) of m_{-1} (which is proportional to α_D). Pictorially, this behavior is best illustrated in the inset of Fig. 5 which displays the “*running*” $m_{-1}(\omega)$ sum. The inset provides a clear indication that both the total m_{-1} moment as well as the fraction contained in the Pygmy resonance are highly sensitive to the neutron-skin thickness of ^{208}Pb . To heighten this sensitivity we display on the right-hand panel of Fig. 5 the *fractional change* in both the total and Pygmy contributions to the m_{-1} moment (i.e., the energy weighted sum rule) and to the dipole polarizability α_D as a function of the neutron skin of ^{208}Pb (we denote these fractional changes with a “*tilde*” in the figure). These results illustrate the strong correlation between the neutron skin and α_D and establish how a combined measurement

of these laboratory observables will be of vital importance in constraining the isovector sector of the nuclear density functional.

5. Conclusions

Measurements of neutron radii provide important constraints on the isovector sector of nuclear density functionals and offer vital guidance in areas as diverse as atomic parity violation, heavy-ion collisions, and neutron-star structure. In this contribution we examined the possibility of using the quintessential nuclear mode—the isovector dipole resonance—as a promising complementary observable. For this mode of excitation in which protons oscillate coherently against neutrons, the symmetry energy acts as its restoring force. Thus, models with a soft symmetry energy predict large values for the symmetry energy at the densities of relevance to the excitation of this mode. As a consequence, softer models generate a dipole response that is both hardened and quenched relative to the stiffer models. However, being protected by the Thomas-Reiche-Kuhn sum rule, the energy weighted sum rule is largely insensitive to this behavior. In contrast, for the inverse energy-weighted sum—which is directly proportional to the electric dipole polarizability α_D —the quenching and hardening act in tandem. Thus, models with a soft symmetry energy predict smaller values of α_D than their stiffer counterparts. This results in a powerful “data-to-data” relation: *the smaller α_D , the thinner the neutron skin*. Moreover, we saw that a significant amount of electric dipole strength is concentrated in the low-energy fragment; the so-called Pygmy resonance.

In summary, motivated by two seminal experiments [33, 55], we examined possible correlations between the electric dipole polarizability and the neutron skin of neutron-rich nuclei. The neutron-skin thickness of a heavy nucleus is a quantity of critical importance for our understanding of a variety of nuclear and astrophysical phenomena. In particular, the neutron-skin thickness of ^{208}Pb can provide stringent constraints on the density dependence of the symmetry energy which, in turn, has a strong impact on the structure, dynamics, and composition of neutron stars. We conclude that precise measurements of neutron skins and α_D —ideally on a variety of nuclei—should significantly constrain the isovector sector of the nuclear energy density functional and will provide critical insights into the nature of neutron-rich matter.

Acknowledgments

This work was supported in part by grant DE-FD05-92ER40750 from the Department of Energy.

References

- [1] The Committee on the Assessment of and Outlook for Nuclear Physics; Board on Physics and Astronomy; Division on Engineering and Physical Sciences; National Research Council, *Nuclear Physics: Exploring the Heart of Matter* (The National Academies Press, 2012), ISBN 9780309260404, URL http://www.nap.edu/openbook.php?record_id=13438.
- [2] Nuclear Science Advisory Committee, *2007 Long Range Plan: The Frontiers of Nuclear Science*, URL <http://science.energy.gov/np/nsac>.
- [3] G. Baym, C. Pethick, and P. Sutherland, *Astrophys. J.* **170**, 299 (1971).
- [4] S. B. Ruester, M. Hempel, and J. Schaffner-Bielich, *Phys. Rev.* **C73**, 035804 (2006).
- [5] X. Roca-Maza and J. Piekarewicz, *Phys. Rev.* **C78**, 025807 (2008).
- [6] X. Roca-Maza, J. Piekarewicz, T. Garcia-Galvez, and M. Centelles (2011a), contribution to the book *Neutron Star Crust* (Nova Publishers), 1109.3011.
- [7] D. G. Ravenhall, C. J. Pethick, and J. R. Wilson, *Phys. Rev. Lett.* **50**, 2066 (1983).
- [8] M. Hashimoto, H. Seki, and M. Yamada, *Prog. Theor. Phys.* **71**, 320 (1984).
- [9] C. J. Horowitz, M. A. Perez-Garcia, and J. Piekarewicz, *Phys. Rev.* **C69**, 045804 (2004a).
- [10] C. J. Horowitz, M. A. Perez-Garcia, J. Carriere, D. K. Berry, and J. Piekarewicz, *Phys. Rev.* **C70**, 065806 (2004b).
- [11] C. J. Horowitz, M. A. Perez-Garcia, D. K. Berry, and J. Piekarewicz, *Phys. Rev.* **C72**, 035801 (2005).

- [12] G. Watanabe, K. Sato, K. Yasuoka, and T. Ebisuzaki, Phys. Rev. **C68**, 035806 (2003).
- [13] G. Watanabe, T. Maruyama, K. Sato, K. Yasuoka, and T. Ebisuzaki, Phys. Rev. Lett. **94**, 031101 (2005).
- [14] G. Watanabe, H. Sonoda, T. Maruyama, K. Sato, K. Yasuoka, et al., Phys. Rev. Lett. **103**, 121101 (2009).
- [15] F. J. Fattoyev, C. J. Horowitz, J. Piekarewicz, and G. Shen, Phys. Rev. **C82**, 055803 (2010).
- [16] G. A. Lalazissis, J. Konig, and P. Ring, Phys. Rev. **C55**, 540 (1997).
- [17] G. A. Lalazissis, S. Raman, and P. Ring, At. Data Nucl. Data Tables **71**, 1 (1999).
- [18] B. G. Todd-Rutel and J. Piekarewicz, Phys. Rev. Lett. **95**, 122501 (2005).
- [19] F. Ozel, G. Baym, and T. Guver, Phys. Rev. **D82**, 101301 (2010).
- [20] A. W. Steiner, J. M. Lattimer, and E. F. Brown, Astrophys. J. **722**, 33 (2010).
- [21] P. Demorest, T. Pennucci, S. Ransom, M. Roberts, and J. Hessels, Nature **467**, 1081 (2010).
- [22] H. Mueller and B. D. Serot, Nucl. Phys. **A606**, 508 (1996).
- [23] C. J. Horowitz and J. Piekarewicz, Phys. Rev. Lett. **86**, 5647 (2001a).
- [24] B. D. Serot and J. D. Walecka, Adv. Nucl. Phys. **16**, 1 (1986).
- [25] B. D. Serot and J. D. Walecka, Int. J. Mod. Phys. **E6**, 515 (1997).
- [26] J. Piekarewicz, Phys. Rev. **C76**, 064310 (2007).
- [27] J. M. Lattimer and M. Prakash, Phys. Rept. **442**, 109 (2007).
- [28] J. Piekarewicz and M. Centelles, Phys. Rev. **C79**, 054311 (2009).
- [29] B. A. Brown, Phys. Rev. Lett. **85**, 5296 (2000).
- [30] R. J. Furnstahl, Nucl. Phys. **A706**, 85 (2002).
- [31] C. J. Horowitz and J. Piekarewicz, Phys. Rev. **C64**, 062802 (2001b).
- [32] X. Roca-Maza, M. Centelles, X. Viñas, and M. Warda, Phys. Rev. Lett. **106**, 252501 (2011b).
- [33] S. Abrahamyan, Z. Ahmed, H. Albatineh, K. Aniol, D. Armstrong, et al., Phys. Rev. Lett. **108**, 112502 (2012).
- [34] C. Horowitz, Z. Ahmed, C. Jen, A. Rakhman, P. Souder, et al., Phys. Rev. **C85**, 032501 (2012).
- [35] T. Donnelly, J. Dubach, and I. Sick, Nucl. Phys. **A503**, 589 (1989).
- [36] P. Danielewicz, Nucl. Phys. **A727**, 233 (2003).
- [37] M. Centelles, X. Roca-Maza, X. Viñas, and M. Warda, Phys. Rev. Lett. **102**, 122502 (2009).
- [38] M. Centelles, X. Roca-Maza, X. Viñas, and M. Warda, Phys. Rev. **C82**, 054314 (2010).
- [39] S. J. Pollock, E. N. Fortson, and L. Wilets, Phys. Rev. **C46**, 2587 (1992).
- [40] T. Sil, M. Centelles, X. Viñas, and J. Piekarewicz, Phys. Rev. **C71**, 045502 (2005).
- [41] M. B. Tsang et al., Phys. Rev. Lett. **92**, 062701 (2004).
- [42] L.-W. Chen, C. M. Ko, and B.-A. Li, Phys. Rev. Lett. **94**, 032701 (2005).
- [43] A. W. Steiner and B.-A. Li, Phys. Rev. **C72**, 041601 (2005).
- [44] D. V. Shetty, S. J. Yennello, and G. A. Souliotis, Phys. Rev. **C76**, 024606 (2007).
- [45] M. B. Tsang et al., Phys. Rev. Lett. **102**, 122701 (2009).
- [46] C. J. Horowitz and J. Piekarewicz, Phys. Rev. **C66**, 055803 (2002).
- [47] J. Carriere, C. J. Horowitz, and J. Piekarewicz, Astrophys. J. **593**, 463 (2003).
- [48] A. W. Steiner, M. Prakash, J. M. Lattimer, and P. J. Ellis, Phys. Rept. **411**, 325 (2005).
- [49] B.-A. Li and A. W. Steiner, Phys. Lett. **B642**, 436 (2006).
- [50] F. J. Fattoyev and J. Piekarewicz, Phys. Rev. **C82**, 025810 (2010).
- [51] K. Paschke, K. Kumar, R. Michaels, P. A. Souder, and G. M. Urciuoli (2012),
URL <http://hallaweb.jlab.org/parity/prex/prexII.pdf>.
- [52] M. N. Harakeh and A. van der Woude, *Giant Resonances-Fundamental High-frequency Modes of Nuclear Excitation* (Clarendon, Oxford, 2001).
- [53] J. Piekarewicz, Phys. Rev. **C83**, 034319 (2011).
- [54] J. Piekarewicz, B. Agrawal, G. Colò, W. Nazarewicz, N. Paar, et al., Phys. Rev. **C85**, 041302(R) (2012).
- [55] A. Tamii et al., Phys. Rev. Lett. **107**, 062502 (2011).
- [56] I. Poltoratska, P. von Neumann-Cosel, A. Tamii, T. Adachi, C. Bertulani, et al. (2012), [arXiv:1203.2155](https://arxiv.org/abs/1203.2155).
- [57] P.-G. Reinhard and W. Nazarewicz, Phys. Rev. **C81**, 051303 (2010).
- [58] F. Fattoyev and J. Piekarewicz, Phys. Rev. **C84**, 064302 (2011).
- [59] F. Fattoyev and J. Piekarewicz, Phys. Rev. **C88**, 015802 (2012).
- [60] Y. Suzuki, K. Ikeda, and H. Sato, Prog. Theor. Phys. **83**, 180 (1990).
- [61] P. Van Isacker and D. D. Nagarajan, M. A. and Warner, Phys. Rev. **C45**, R13 (1992).
- [62] I. Hamamoto, H. Sagawa, and X. Z. Zhang, Phys. Rev. **C53**, 765 (1996).
- [63] I. Hamamoto, H. Sagawa, and X. Z. Zhang, Phys. Rev. **C57**, R1064 (1998).
- [64] D. Vretenar, N. Paar, P. Ring, and G. A. Lalazissis, Phys. Rev. **C63**, 047301 (2001a).
- [65] D. Vretenar, N. Paar, P. Ring, and G. A. Lalazissis, Nucl. Phys. **A692**, 496 (2001b).
- [66] N. Paar, T. Niksic, D. Vretenar, and P. Ring, Phys. Lett. **B606**, 288 (2005).
- [67] J. Piekarewicz, Phys. Rev. **C73**, 044325 (2006).